RAD51C facilitates checkpoint signaling by promoting CHK2 phosphorylation

Sophie Badie, Chunyan Liao, Maria Thanasoula, Paul Barber, Mark A. Hill, and Madalena Tarsounas

Cancer Research UK/Medical Research Council Gray Institute for Radiation Oncology and Biology, University of Oxford, Oxford OX3 7DQ, England, UK

The RAD51 paralogues act in the homologous recombination (HR) pathway of DNA repair. Human RAD51C (hRAD51C) participates in branch migration and Holliday junction resolution and thus is important for processing HR intermediates late in the DNA repair process. Evidence for early involvement of RAD51 during DNA repair also exists, but its function in this context is not understood. In this study, we demonstrate that RAD51C accumulates at DNA damage sites concomitantly with the RAD51 recombinase and is retained after RAD51 disassembly, which is consistent with both an early and a late function for RAD51C. RAD51C recruitment depends on ataxia telangiectasia mutated, NBS1, and replication protein A, indicating it functions after DNA end resection but before RAD51 assembly. Furthermore, we find that RAD51C is required for activation of the checkpoint kinase CHK2 and cell cycle arrest in response to DNA damage. This suggests that hRAD51C contributes to the protection of genome integrity by transducing DNA damage signals in addition to engaging the HR machinery.

Introduction

The cell's ability to survive DNA damage relies on the action of DNA damage response pathways that delay DNA replication, halt progression into mitosis, and engage the DNA repair machinery. Central to the response to double-stranded DNA breaks (DSBs) are two kinases, ataxia telangiectasia mutated (ATM) and ATM related (ATR), which are members of the phosphatidylinositol-3 kinase–like family. These are recruited to DSBs and single-stranded DNA (ssDNA), respectively, to phosphorylate key substrates required for cell cycle control and activation of DNA repair pathways (for reviews see Shiloh, 2003; Bartek and Lukas, 2007). During S phase or G2 phase, recruitment of the MRE11–RAD50–NBS1 (MRN) complex to DSBs (Petrini and Stracker, 2003) is thought to trigger ATM phosphorylation, which activates two parallel signaling pathways, leading to cell cycle arrest and initiation of homologous recombination (HR; Jazayeri et al., 2006). The checkpoint effector kinase CHK2 is phosphorylated in an ATM- and NBS1-dependent manner (Matsuoka et al., 1998, 2000; Buscemi et al., 2001) to trigger its activation. In a parallel pathway, the MRN-dependent resection of the broken DNA ends generates ssDNA overhangs, the substrate for DNA repair reactions by HR. Replication protein A (RPA) assembly onto these ssDNA tails triggers ATR-dependent signaling and activation of the CHK1 checkpoint kinase (Zou and Elledge, 2003; Garcia-Muse and Boulton, 2005; Adams et al., 2006; Cuadrado et al., 2006; Jazayeri et al., 2006; Myers and Cortez, 2006). CHK1 and CHK2 delay cell cycle progression, in part by inhibiting Cdk activity, which in turn facilitates HR initiation by RAD51 filament assembly (West, 2003).

A central role in the process of HR is played by the RAD51 recombinase (West, 2003). In mammalian cells, a recently characterized family of proteins known as the RAD51 paralogues consists of five proteins (RAD51B, RAD51C, RAD51D, XRCC2, and XRCC3) related to each other and to RAD51 itself. Their precise cellular function remains unknown. Cells lacking the RAD51 paralogues are defective in gene targeting and exhibit a genomic instability phenotype and high sensitivity to ionizing radiation (IR) and DNA cross-linking agents, which are indicative of their role in recombinational DNA repair (Liu et al., 1998; Takata et al., 2001; French et al., 2002). The paralogues form complexes with each other (Masson et al., 2001; Miller et al., 2002; Wiese et al., 2002). Specific subcomplexes are thought to perform distinct cellular functions. RAD51C and XRCC3 but not the other paralogues are part of a complex that possesses branch migration and Holliday junction resolution

Correspondence to Madalena Tarsounas: madalena.tarsounas@rob.ox.ac.uk

Abbreviations used in this paper: ATM, ataxia telangiectasia mutated; ATR, ATM related; CENP-F, centromeric protein F; DSB, double-stranded DNA break; HR, homologous recombination; hRAD51C, human RAD51C; HU, hydroxyurea; IR, ionizing radiation; MEF, mouse embryonic fibroblast; MRN, MRE11–RAD50–NBS1; RPA, replication protein A; shRNA, short hairpin RNA; ssDNA, single-stranded DNA.

The Rockefeller University Press $30.00
J. Cell Biol. Vol. 185 No. 4 587–600
www.jcb.org/cgi/doi/10.1083/jcb.200811079

activities (Liu et al., 2004, 2007). RAD51D, another member of the RAD51 paralogue family, associates with telomeres in meiotic and somatic cells, and its capping function at telomeres is essential for telomere integrity (Tarsounas et al., 2004b). In addition, a role for RAD51C, XRCC2, and XRCC3 in chromosome segregation and centrosome integrity has been proposed (Griffin et al., 2000; Renglin Lindh et al., 2007).

A prominent cytological consequence of DNA damage and checkpoint activation is the accumulation of DNA repair and signaling proteins at the sites of damage that can be visualized microscopically as nuclear foci. In response to IR, RAD51 assembles at DSB sites with well-defined kinetics and molecular requirements (Haaf et al., 1995; Scully et al., 1997). The formation and stability of RAD51 foci is dependent on the presence of BRCA2 and the five RAD51 paralogues (Yuan et al., 1999; Takata et al., 2001; French et al., 2002; Godthelp et al., 2002; Tarsounas et al., 2003, 2004a). This observation, together with the ability of RAD51 to directly interact with both RAD51C and BRCA2 (Chen et al., 1998b; Wong et al., 1997; Rodrigue et al., 2006), led to the concept that these proteins function as cofactors for RAD51 assembly after ssDNA resection at DSB sites. However, although the role of BRCA2 as RAD51 loader is supported by both biochemical and cell biological data, the association of the RAD51C–XRCC3 complex with Holliday junction processing activities suggested that the latter proteins may fulfill a role in the late steps of HR, downstream of RAD51. How RAD51C acts during the early steps of HR and how it promotes RAD51 assembly remain unknown.

In this study, we report that human RAD51C (hRAD51C) is recruited to damage sites in response to treatment with IR or the replication inhibitor hydroxyurea (HU). The kinetics of RAD51C recruitment is consistent with both an early and a late role in HR. We further identify an early function of RAD51C in DNA repair in facilitating phosphorylation of the checkpoint kinase CHK2 and thereby transduction of the damage signal, leading to cell cycle arrest and HR activation. Our data identify RAD51C as a DNA damage response factor required for the activation of S and G2/M checkpoints, which could contribute to the early steps of recombinational DNA repair.

Results

hRAD51C accumulates at DSBs

A major limitation in defining the cellular functions of RAD51 paralogues was the lack of antibodies sensitive enough to visualize these proteins, which were thought to be expressed at low levels in the cell. In this work, we purified a monoclonal antibody raised against full-length RAD51C (Masson et al., 2001) from hybridoma cell supernatants, avoiding a low pH elution step (see Materials and methods). This antibody reacted with a single major band of the expected size for RAD51C in extracts of HeLa and U2OS human cells (Fig. 1 A). No obvious change in the abundance or migration of the RAD51C protein was detected in whole cell extracts after treatment with IR.

To investigate the role of RAD51C in DSB repair, human cell lines (HeLa and U2OS) were subjected to 10 Gy of IR, and RAD51C subcellular localization was determined using indirect immunofluorescence. After irradiation, a significant portion of cells showed numerous RAD51C foci, whereas no signal was detected in nonirradiated control cells (Fig. 1 B). RAD51C foci were detected after irradiation with doses as low as 1 Gy (Fig. S1). They were also detected in several other human cell lines (WI38 and HCT116), but the antibody was not able to efficiently visualize RAD51C foci in mouse fibroblasts (unpublished data). Treatment of human cells with two different siRNAs against RAD51C efficiently reduced the expression of this protein, as detected by immunoblotting (Fig. 1 C). Consistent with this, irradiated cells that had been depleted of RAD51C were impaired in their ability to form RAD51C foci, which is in contrast to cells treated with control siRNA (Fig. 1 D). To further test the specificity of the RAD51C monoclonal antibody, we established single-cell clones stably expressing hRAD51C from an siRNA-resistant cDNA construct (RAD51C*; Fig. S2 A). In irradiated cells transfected with vector only, RAD51C depletion by siRNA abrogated formation of DNA repair foci. However, in cells harboring the siRNA-resistant RAD51C*, RAD51C foci formation in response to IR remained intact. This demonstrates that the anti-RAD51C antibody specifically recognized accumulation of the RAD51C protein into DNA damage–induced foci.

To confirm this localization pattern, we established single-cell clones stably expressing N-terminally GFP-tagged hRAD51C (Rodrigue et al., 2006) at levels comparable with the endogenous protein. In response to partial irradiation of nuclei with ultrasoft x rays (~2 Gy averaged over the cell), GFP-RAD51C accumulated into foci that overlapped with RAD51 (Fig. S2 B). Preferential localization of the GFP-RAD51C foci in broad stripes within the nuclei, generated by the x-ray mask, further confirms its accumulation at sites of DNA damage.

RAD51C foci colocalize with RAD51 but persist during DSB repair

RAD51C is required for DSB repair by HR, and a direct protein–protein interaction of RAD51C with the RAD51 recombinase has been reported (Rodrigue et al., 2006). This suggested that the two proteins act together in the HR pathway. To investigate whether this was the case, irradiated HeLa cells were costained with mouse anti-RAD51C and rabbit anti-RAD51 antibodies (Fig. 1, E and F). Some of the cells contained mainly RAD51C foci (Fig. 1 E, red circle) or RAD51 foci (Fig. 1 E, green circle), whereas others contained both types of foci that partly colocalized (65% of RAD51C foci colocalized with RAD51, as determined by visual inspection; Fig. 1 E, yellow circle). This pattern suggests that RAD51C and RAD51 play overlapping but not identical roles in response to irradiation.

Detection of cells showing exclusively RAD51C or RAD51 staining and of cells in which both proteins colocalized suggested that the two activities assemble sequentially at the sites of damage. To test this, we monitored the assembly of RAD51C and RAD51 foci in response to radiation-induced DNA damage in a time course experiment (Fig. 2 A). RAD51 is known to form spontaneous foci even in the absence of DNA damage, which is a feature not shared by RAD51C (Fig. 1 B). These foci are thought to represent stalled replication forks during cell cycle progression through S phase (Tarsounas et al., 2003). The blue line in Fig. 2 A indicates the frequency of spontaneous

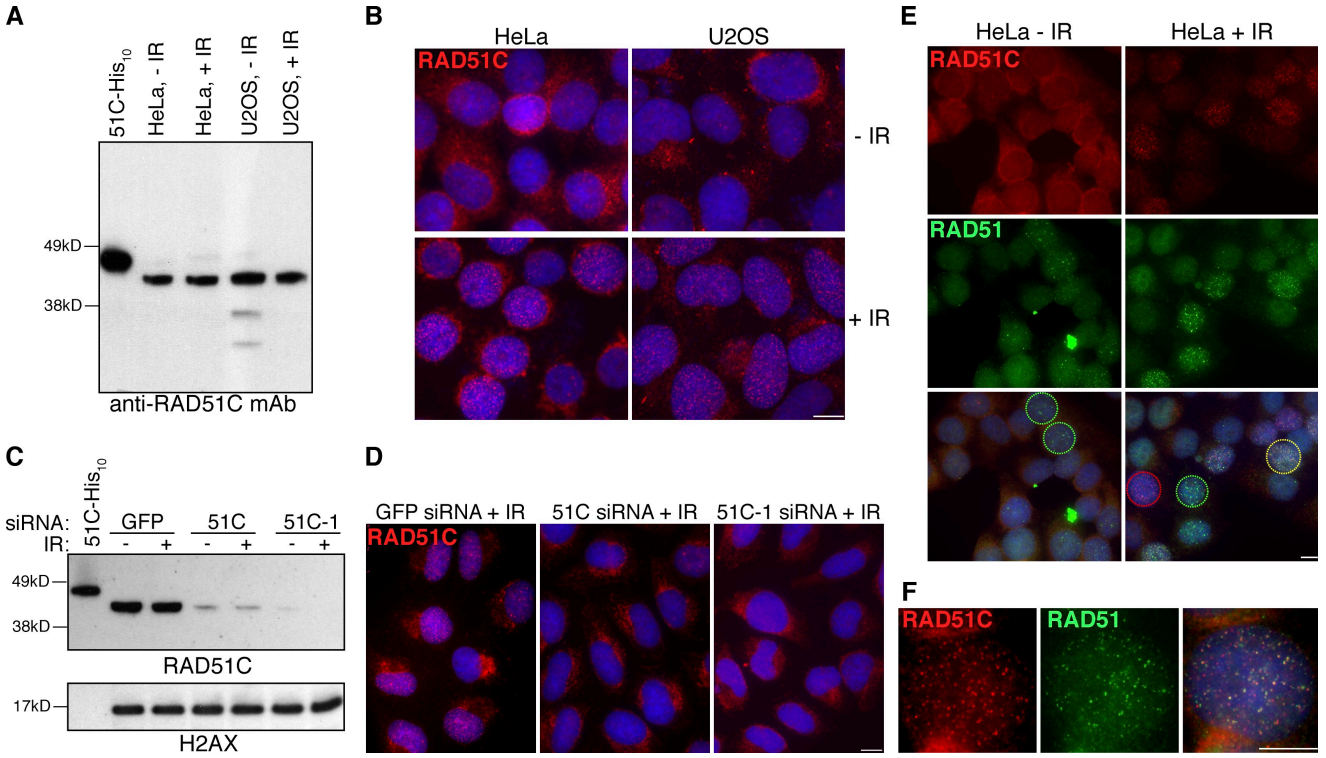

Figure 1. **hRAD51C forms nuclear foci in response to IR.** (A) Western blot detection of hRAD51C. An immunoblot of extracts prepared from irradiated and nonirradiated HeLa and U2OS cells was probed with anti-hRAD51C antibody. Recombinant hRAD51C-His_{10}, migrating more slowly because of its epitope tag, served as a control. (B) Immunofluorescence detection of RAD51C in paraformaldehyde-fixed HeLa and U2OS cells. Irradiated (10 Gy) and nonirradiated cultures were stained with anti-hRAD51C monoclonal antibody (red) 2 h after treatment. DNA was counterstained with DAPI (blue). (C) siRNA-mediated reduction of RAD51C expression. Cells were transfected with control or RAD51C siRNA and irradiated 48 h after transfection. Cell extracts, prepared 2 h after irradiation, were analyzed by Western blotting. (D) siRNA-mediated reduction of RAD51C foci. As in C, but cells were fixed 2 h after IR and stained with anti-hRAD51C monoclonal antibody (red). Image acquisition parameters were identical for the three samples. (E) Partial colocalization of RAD51C and RAD51 in irradiated HeLa cells stained with anti-RAD51C (red) and anti-RAD51 antibodies (green). Nuclei displaying only RAD51C or RAD51 foci or containing both types of foci are labeled with a red, green, or yellow circle, respectively. (F) Enlarged image of a cell containing both RAD51C (red) and RAD51 foci (green). Bars, 10 μm.

RAD51 foci in nonirradiated control cells. This value was subtracted from the total number of RAD51-positive cells after irradiation. At early time points after irradiation, RAD51C and RAD51 foci appeared with similar kinetics. Although RAD51 foci peaked at 1 h after treatment, RAD51C-positive cells further increased in number and persisted until 6 h after damage. Representative images in Fig. 2 B illustrate these changes. To further characterize the relative kinetics of appearance of the two types of foci, we computationally determined the number of foci in the nuclei of a population of cells (see Materials and methods; Fig. 2 C). This analysis revealed that the number of RAD51C foci per nucleus increased over time and persisted even 6 h after irradiation (Fig. 2 D). In contrast, the number of RAD51 foci per cell already reached a peak 40 min after irradiation and decreased over time (Fig. 2 E), with kinetics similar to that of manually scored RAD51-positive cells (Fig. 2 A). These data are consistent with the possibility that RAD51C acts both at the early stages of DSB processing as well as after RAD51-mediated HR reactions have been completed.

Further evidence for an early role of RAD51C during HR

An early role for RAD51C in DNA repair has been suggested by observations that RAD51C-defective hamster and chicken cells do not assemble RAD51 foci in response to DNA damage (Takata et al., 2000; French et al., 2002). This led to the concept that RAD51C acts before RAD51 in the HR pathway. Consistent with this, we found that hRAD51C foci precede RAD51 foci formation induced after release from HU treatment (Fig. 3 A). In a subset of the cells (20–30%; Fig. 3 B), RAD51C foci became detectable within 6 min after removal of HU, a time when RAD51 foci were not present. 4 h after the release, both RAD51 and RAD51C foci were present in 50–60% of cells, in which they partly colocalized, which is indicative of recombinational activity during replication fork restart.

Loading of RAD51 at sites of DNA damage in the HR pathway requires the tumor suppressor BRCA2 (Davies et al., 2001). This is thought to be mediated by the ability of BRCA2 to recruit RAD51 monomers and promote their assembly into a RAD51 filament at DSBs. Human CAPAN-1 cells derived from a human pancreatic tumor (Goggins et al., 1996; Chen et al., 1998a) express a truncated form of the BRCA2 protein, which compromises their ability to assemble RAD51 foci in response to irradiation. In contrast, RAD51C foci formation after irradiation was not affected by loss of BRCA2 function (Fig. 3 C). This provides further evidence that RAD51C plays a distinct and earlier role than RAD51 at DSBs.

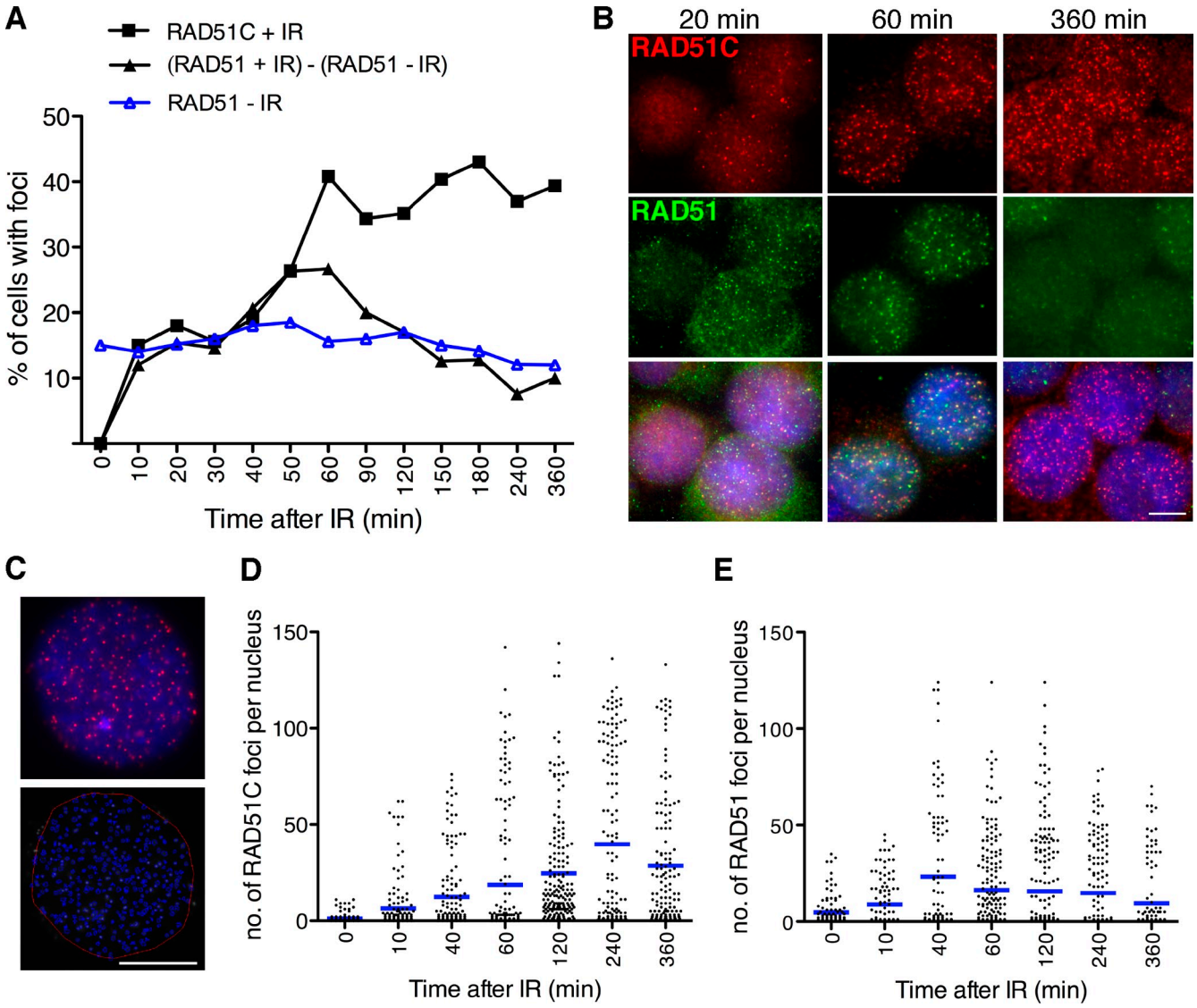

Figure 2. **Distinct kinetics of RAD51C and RAD51 foci formation.** HeLa cells were fixed at the indicated time points after 10 Gy of irradiation and stained with anti-RAD51C (red) and anti-RAD51 antibodies (green). DNA was stained with DAPI (blue). (A) More than 100 cells were scored at each time point. Nuclei containing >5 foci were counted as positive. The level of spontaneous RAD51 foci in nonirradiated cells (RAD51 − IR) is indicated in blue and was subtracted from the number of IR-induced RAD51 foci (RAD51 + IR). (B) Representative images of cells at 20, 60, and 360 min after IR. (C) An example of a DAPI-stained nucleus (blue) with RAD51C foci (red) processed using TRI2 software. The computer-generated image delineates the nucleus (red) and individual foci (blue). (D and E) Computational analysis of RAD51 and RAD51C foci in at least 100 cells at the indicated time points after IR. The blue lines indicate the mean number of foci per cell. Bars, 10 µm.

RAD51C foci form in S or G2 phase

During the aforementioned experiments, we noticed that not all cells exposed to irradiation developed visible RAD51C foci. This could indicate that RAD51C recruitment to DSBs occurs during certain stages of the cell cycle but not others. As HR is known to act predominantly during S and G2, we used centromeric protein F (CENP-F) staining to identify these cells. CENP-F has a nuclear diffuse distribution from S phase onwards, becomes more intense in G2 phase (Fletcher et al., 2003), and shows specific concentration at kinetochores during mitosis. The appearance of nuclear RAD51C foci followed a similar pattern in U2OS cells. Radiation-induced foci were detectable in cells displaying weak CENP-F staining (Fig. 4 A) and reached greater intensity in cells with strong CENP-F. This suggests that RAD51C foci specifically form during S or G2 phase but not G1 phase of the cell cycle.

ATM and NBS1 are required for RAD51C assembly at DSBs

Repair of DSBs in S and G2 is controlled by the ATM pathway (Jazayeri et al., 2006). Therefore, we analyzed whether RAD51C recruitment to damage sites depends on ATM. We treated U2OS cells with caffeine, which is an inhibitor of the ATM and ATR members of the phosphatidylinositol-3 kinase–like family. This diminished RAD51C foci formation after irradiation (Fig. S3), suggesting that the RAD51C response is regulated by ATM and/or ATR. To test the dependence of RAD51C recruitment specifically on ATM, we monitored the cellular response to Ku55933,

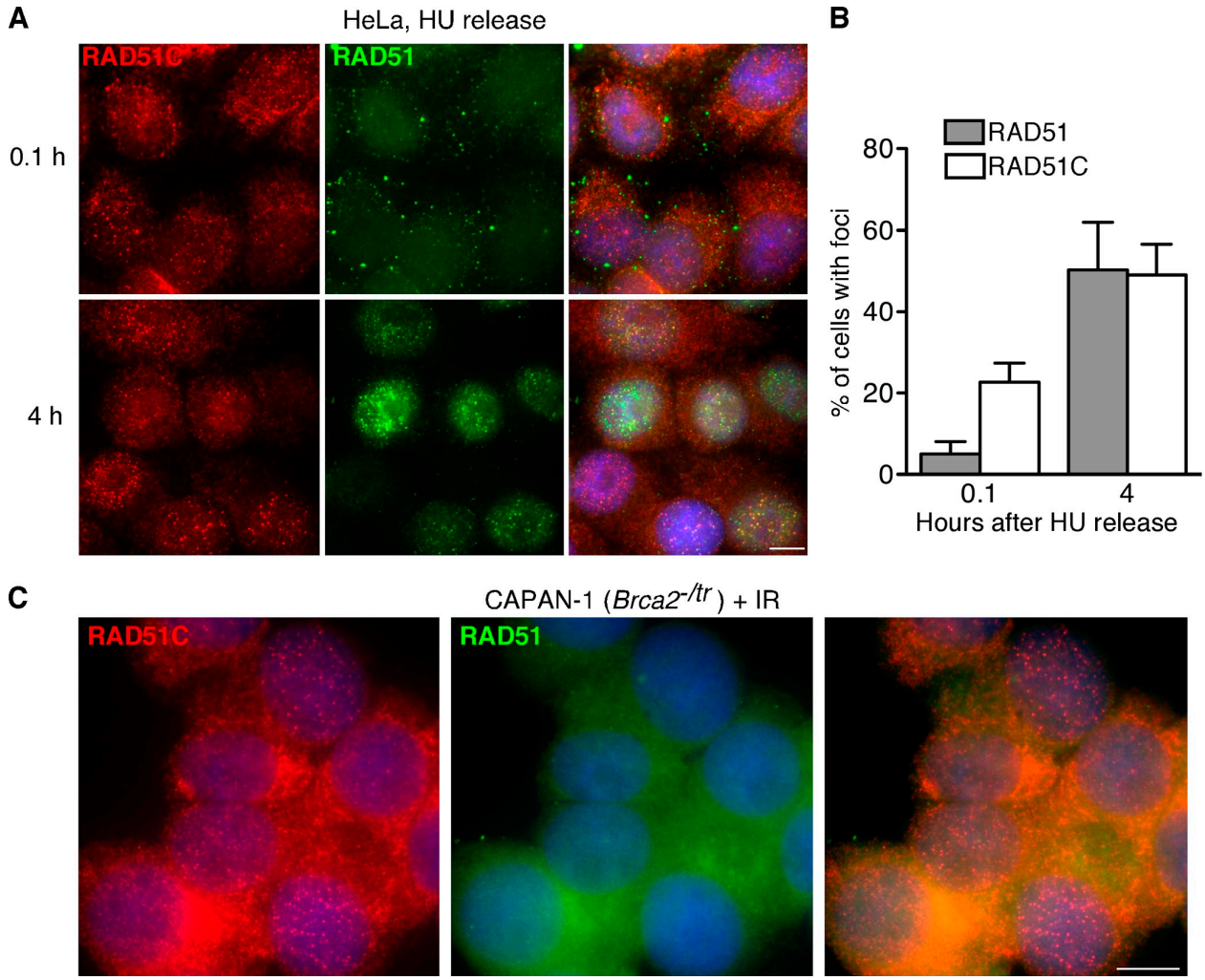

Figure 3. **RAD51C assembles before and independently of RAD51 at sites of DNA damage.** (A) HeLa cells were incubated with 2 mM HU for 17 h and then released into fresh medium. Cells were fixed 0.1 or 4 h after release and stained with anti-RAD51C (red) and anti-RAD51 antibodies (green). (B) For each of the two samples in A, at least 100 cells were examined for the presence of RAD51 or RAD51C foci. The mean and standard deviations of three independent experiments are shown. (C) CAPAN-1 (*Brca2*$^{-/tr}$) cells were irradiated (10 Gy), fixed 2 h after irradiation, and stained with anti-RAD51C (red) and anti-RAD51 antibodies (green). Bars, 10 µm.

an ATM-specific inhibitor (Hickson et al., 2004), after irradiation. This treatment inhibited formation of RAD51C foci (Fig. 4 B), whereas cells treated with solvent (DMSO) were not affected. Furthermore, when cells of a fibroblast cell line derived from an ataxia telangiectasia patient that is deficient in ATM function were irradiated, only 3.2% of the cells formed RAD51C foci. The level of RAD51C foci formation was restored to 28.1% of the cells by transfection of a complementing vector encoding wild-type ATM (Fig. 4 C), suggesting that ATM activity is required for efficient RAD51C recruitment to sites of DNA damage.

The MRN complex is thought to activate ATM at DNA break sites. Therefore, we examined RAD51C recruitment to sites of DNA damage in NBS1-deficient Nijmegen breakage syndrome fibroblasts. Nijmegen breakage syndrome cells complemented with full-length NBS1 were proficient in RAD51C focus formation in response to IR, but cells lacking NBS1 were not (Fig. 4, D and E). These results indicate that the recruitment of RAD51C requires both functional ATM and NBS1. We also visualized RPA foci as a control in these experiments and confirmed that ATM and NBS1 are required for radiation-induced RPA assembly at DSBs (Jazayeri et al., 2006). This indicated that RAD51C is regulated by the ATM pathway, similarly to RPA.

RAD51C accumulation at damage sites depends on RPA

The ATM and NBS1 dependence of both RAD51C and RPA recruitment to damage sites prompted us to test whether both proteins colocalized in response to DNA damage. Indeed, RAD51C and RPA foci closely overlapped in all cells after both irradiation and release from HU treatment (Fig. 5 A). RPA binds ssDNA generated during MRN complex–dependent strand resection. To see whether RAD51C affects strand resection, we analyzed RPA foci formation in cells depleted of RAD51C. RPA assembled normally in response to irradiation, both in cells treated with RAD51C and control siRNAs (Fig. 5 B). As a control, formation of RAD51 foci was efficiently prevented by RAD51C-depletion under our conditions, as previously reported (French et al., 2002; Rodrigue et al., 2006). Conversely, down-regulation

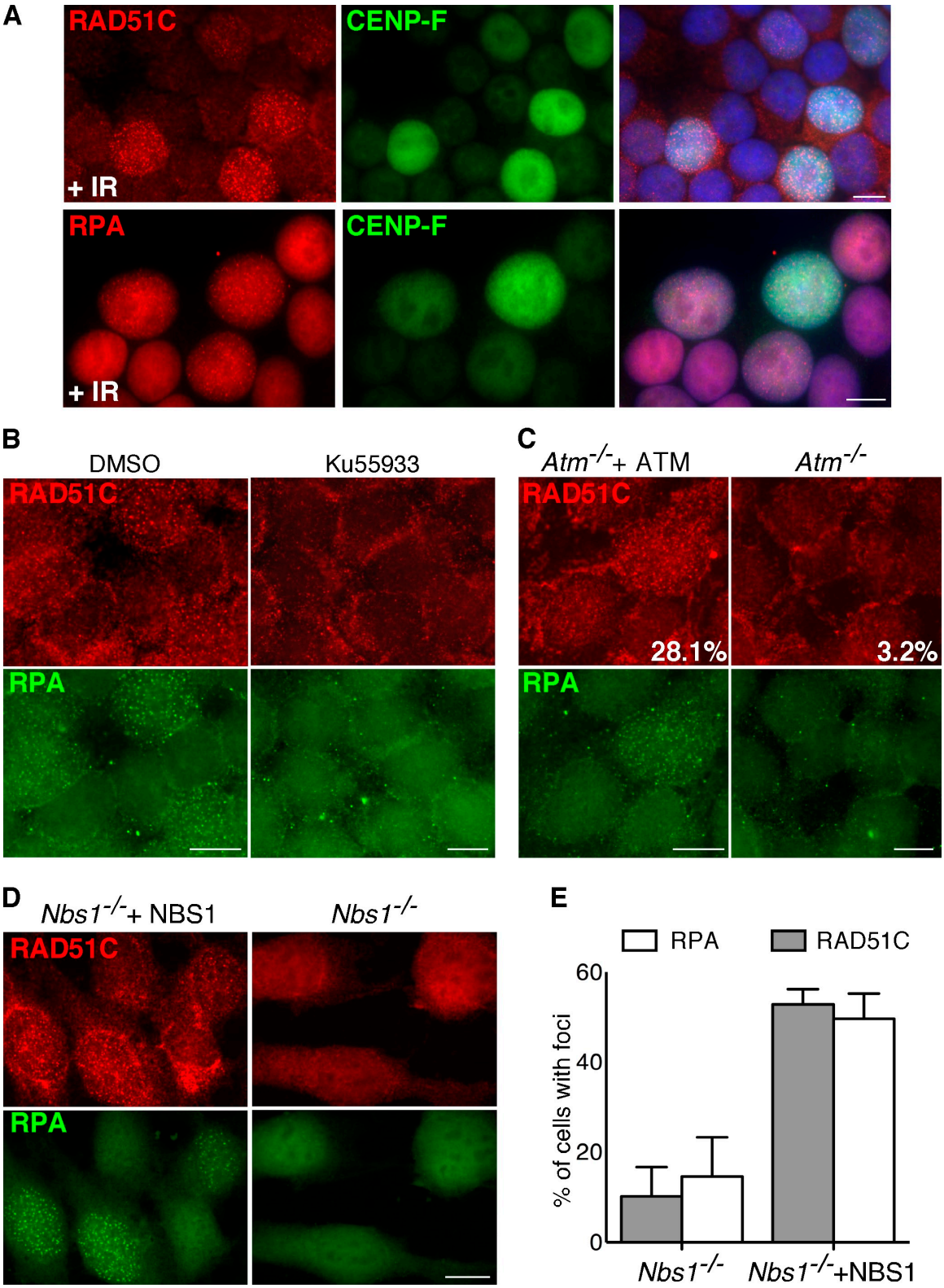

Figure 4. **RAD51C accumulation at DNA lesions in S/G2 requires ATM and NBS1.** (A) U2OS cells were irradiated (10 Gy of IR), fixed after 2 h, and stained with anti-RAD51C or anti-RPA (red) and anti–CENP-F antibodies (green). Nuclei were visualized with DAPI (blue). (B) U2OS cells were treated with ATM inhibitor (Ku55933) or solvent (DMSO) and then irradiated (10 Gy), fixed 2 h later, and stained with anti-RAD51C (red) and anti-RPA antibodies (green). (C) *Atm*-deficient cells stably transfected with a vector expressing full-length ATM or an empty vector were treated and processed as in B. (D) *Nbs1*-deficient cells stably transfected with a vector expressing full-length NBS1 or an empty vector were treated and stained as in B. (E) The percentage of nuclei exhibiting RAD51C or RPA foci was determined for at least 100 cells from D. The mean and standard deviation of three independent experiments are shown. Bars, 10 μm.

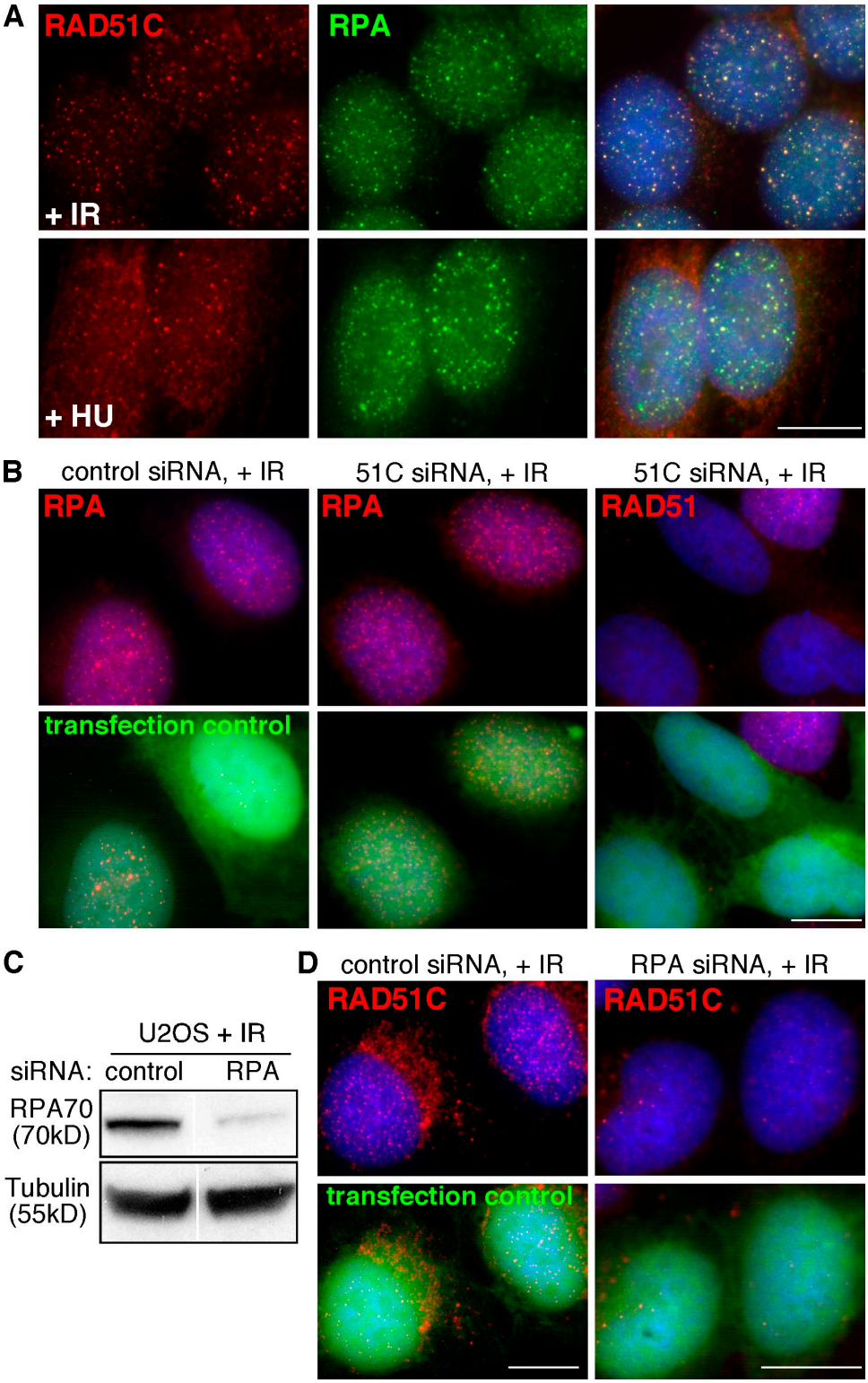

Figure 5. **RAD51C assembly at break sites depends on RPA.** (A) HeLa cells were irradiated (10 Gy) and fixed 2 h later or treated with 2 mM HU for 17 h, released into fresh media, and fixed 4 h after release. Cells were stained with anti-RAD51C (red) and anti-RPA antibodies (green). Nuclei were visualized with DAPI (blue). (B) Control or RAD51C siRNA was cotransfected with a GFP-expressing vector. U2OS cells were irradiated 48 h after transfection, fixed after 2 h, and stained with anti-RPA and anti-RAD51 antibodies (red). (C) siRNA-mediated reduction of RPA expression. Cells were transfected with control or RPA siRNA and irradiated 48 h after transfection. Cell extracts were analyzed by Western blotting against RPA and tubulin. (D) Control or RPA siRNA was cotransfected with a GFP-expressing vector into U2OS cells. Cells were irradiated 48 h after transfection, fixed after 2 h, and stained against RAD51C. Bars, 10 μm.

of RPA expression completely abolished RAD51C foci formation (Fig. 5, C and D). These data establish that RAD51C colocalizes with RPA and requires RPA binding to ssDNA for its recruitment. Therefore, RAD51C is likely recruited to sites of DSBs after ATM- and NBS1-dependent strand resection and RPA association but before RAD51 filament assembly. How RPA promotes RAD51C recruitment is currently not known. Coimmunoprecipitation experiments did not provide evidence for a direct interaction between the two proteins (Fig. S4).

RAD51C is required for the checkpoint response to DNA damage

In addition to its role in DNA repair, RPA is required for checkpoint activation to halt cell cycle progression in response to damage (Zou and Elledge, 2003; Jazayeri et al., 2006). Therefore, we analyzed whether RAD51C might also be required for the DNA damage checkpoint response. We transfected U2OS cells with either control siRNA or RAD51C-specific siRNA, irradiated the cells 48 h after transfection, and analyzed their cell cycle distribution by FACS analysis 2 h thereafter. RAD51C-proficient cells accumulated in S phase after irradiation with 1 Gy, whereas RAD51C-depleted cells failed to do so and instead showed an increase in G2/M-phase DNA content (Fig. 6 A). No statistically significant differences were found between GFP- and RAD51C siRNA–treated cells in the absence of IR. This suggests that RAD51C is required to delay cell cycle progression through S phase in response to DNA damage. Furthermore, control cells showed a reduction in the frequency of mitotic cells positive for phosphorylated histone H3 after irradiation (Fig. 6 B), which is indicative of arrest at the G2/M transition in the presence of unrepaired DNA lesions. Also this arrest was significantly less pronounced in RAD51C-depleted cells, suggesting compromised control of G2/M progression. In addition, we found that primary mouse embryonic fibroblasts (MEFs), in which RAD51C expression was inhibited using retrovirally delivered short hairpin RNA (shRNA), entered mitosis in spite of the presence of unrepaired chromatid and chromosome DNA breaks (Fig. 6, C and D). A marked increase in chromatid and chromosome breaks in response to RAD51C depletion was observed in MEFs obtained from two littermate embryos (Fig. 6 E), which is indicative of a DNA repair defect and lack of checkpoint control of progression into mitosis.

RAD51C inhibition results in reduced CHK2 phosphorylation

To gain insight into the mechanism by which RAD51C mediates checkpoint integrity, cells depleted of RAD51C were assessed for their ability to phosphorylate and thereby activate the downstream checkpoint kinases CHK1 and CHK2 in response to damage. In U2OS cells exposed to a radiation dose of 10 Gy, RAD51C depletion did not affect phosphorylation of CHK1 on Ser 317 (Fig. 7 A). Instead, it caused reproducible reduction in CHK2 phosphorylation on Thr 68. CHK2 is phosphorylated and activated by ATM in response to damage (Matsuoka et al., 2000). To analyze whether phosphorylation of other ATM targets in addition to CHK2 was impaired in the absence of RAD51C, we analyzed phosphorylation of the ATM substrate SMC1. Unlike CHK2, SMC1 phosphorylation remained unaffected in the absence of RAD51C. ATM autophosphorylation, which is indicative of activation of this kinase in response to DNA damage, was also unaltered by RAD51C depletion (Fig. 7 A).

The impaired CHK2 response in the absence of RAD51C became more pronounced in cells exposed to a lower radiation dose (1 Gy; Fig. 7 B), whereas CHK1 phosphorylation again remained unaffected. Similar results were obtained with HeLa cells exposed to the same dose of IR (Fig. 7 C). Additionally, depletion of RAD51C from U2OS cells with a second siRNA (RAD51C-1) also led to a reduction in CHK2 phosphorylation (Fig. S5 A). Consistent with a RAD51C requirement for efficient checkpoint response, RAD51C-depleted MEFs that entered mitosis with unrepaired DNA breaks also lacked CHK2 activation (Fig. S5 B).

RAD51C is a component of three distinct RAD51 paralogue complexes in human cells. A complex formed by RAD51C and XRCC3 has been shown to interact with RAD51 (Rodrigue et al., 2006). Although biochemical analyses suggested that this complex acts in the late stages of HR when Holliday junction intermediates are formed, XRCC3 was also reported to assemble at sites of DNA breaks before RAD51 (Forget et al., 2004). Thus, we tested whether XRCC3 is also required for CHK2 phosphorylation in response to DNA damage. Depletion of XRCC3 using two different siRNAs diminished CHK2 phosphorylation in response to 1 Gy of IR, similarly to RAD51C depletion (Fig. 7 D). This suggests that XRCC3 together with, and probably in complex with, RAD51C promotes checkpoint activation at sites of DSBs. In a similar experiment, depletion of RAD51 did not compromise CHK2 phosphorylation (Fig. S5 C). This is consistent with the possibility that RAD51C and XRCC3 function in CHK2 activation independently of RAD51 filament assembly. CHK2 phosphorylation was detected in nonirradiated RAD51-depleted cells, confirming a DNA repair defect in these cells.

RAD51C foci formation in response to IR was unaffected in *Chk2*$^{-/-}$ cells (Fig. 7 E), indicating a role for RAD51C upstream of this checkpoint kinase. These results suggest that RAD51C is required for ATM-dependent phosphorylation and activation of CHK2. In turn, reduced CHK2 activation could explain the compromised ability of RAD51C-deficient cells to arrest cell cycle progression in response to DNA damage.

Discussion

Evidence for early and late roles for RAD51C in HR

RAD51C is essential for the HR pathway of DNA repair. However, its relationship to RAD51, the central HR activity in mammalian cells, has been subject to controversy. Several lines of evidence support the notion that RAD51C plays a role in promoting RAD51 nucleoprotein filament assembly early during HR: (a) *Rad51c*-deficient hamster, chicken, and human cell lines lack the ability to form IR-induced RAD51 foci (Takata et al., 2001; French et al., 2002; Bennett and Knight, 2005); (b) overexpression of RAD51 can partially rescue the DNA repair defect of *Rad51c*-defective chicken DT40 cells (Takata et al., 2001); (c) the human RAD51B–RAD51C complex functions as

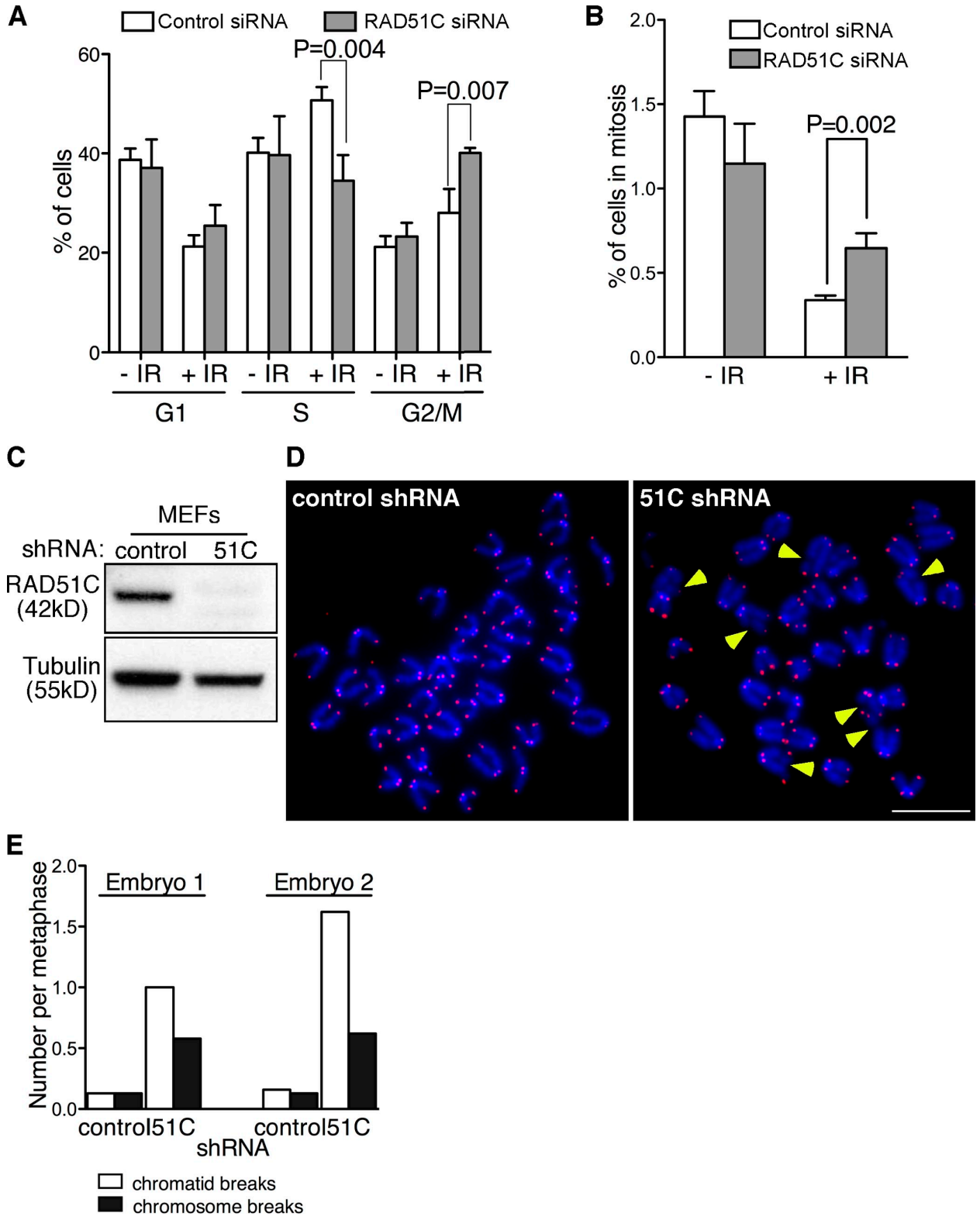

Figure 6. **RAD51C promotes cell cycle arrest in response to DNA damage.** (A) RAD51C depletion reduces IR-induced S-phase delay. U2OS cells were irradiated (1 Gy) 48 h after transfection with control or RAD51C siRNA and, 2 h later, fixed for propidium iodide staining and flow cytometry. G1, S, and G2/M populations were assigned using CellQuest. (B) Analysis of the G2/M checkpoint. As in A, but cells were stained with an antibody against phosphorylated histone H3 and propidium iodide. (A and B) The mean and standard deviation from three independent experiments are shown. Significance in difference between the grouped values was tested using an unpaired *t* test. (C) shRNA-mediated reduction of RAD51C expression in primary MEFs. Cells were infected twice at 12-h intervals with retroviruses expressing control or RAD51C shRNA and then selected with puromycin for 48 h. Cell extracts prepared 3 d after the first infection were analyzed by Western blotting against mouse RAD51C and tubulin. (D) Cells treated as in C were incubated with colcemid for 4 h and processed for FISH analysis of metaphase chromosome spreads with a Cy3-conjugated telomeric peptide nucleic acid probe (red). Arrowheads point to chromatid breaks. (E) Quantification of chromatid and chromosome break frequencies in metaphase spreads from MEFs established from two littermate embryos, each transfected with either control or RAD51C shRNA. 30–50 metaphases were analyzed for each sample. Bar, 10 μm.

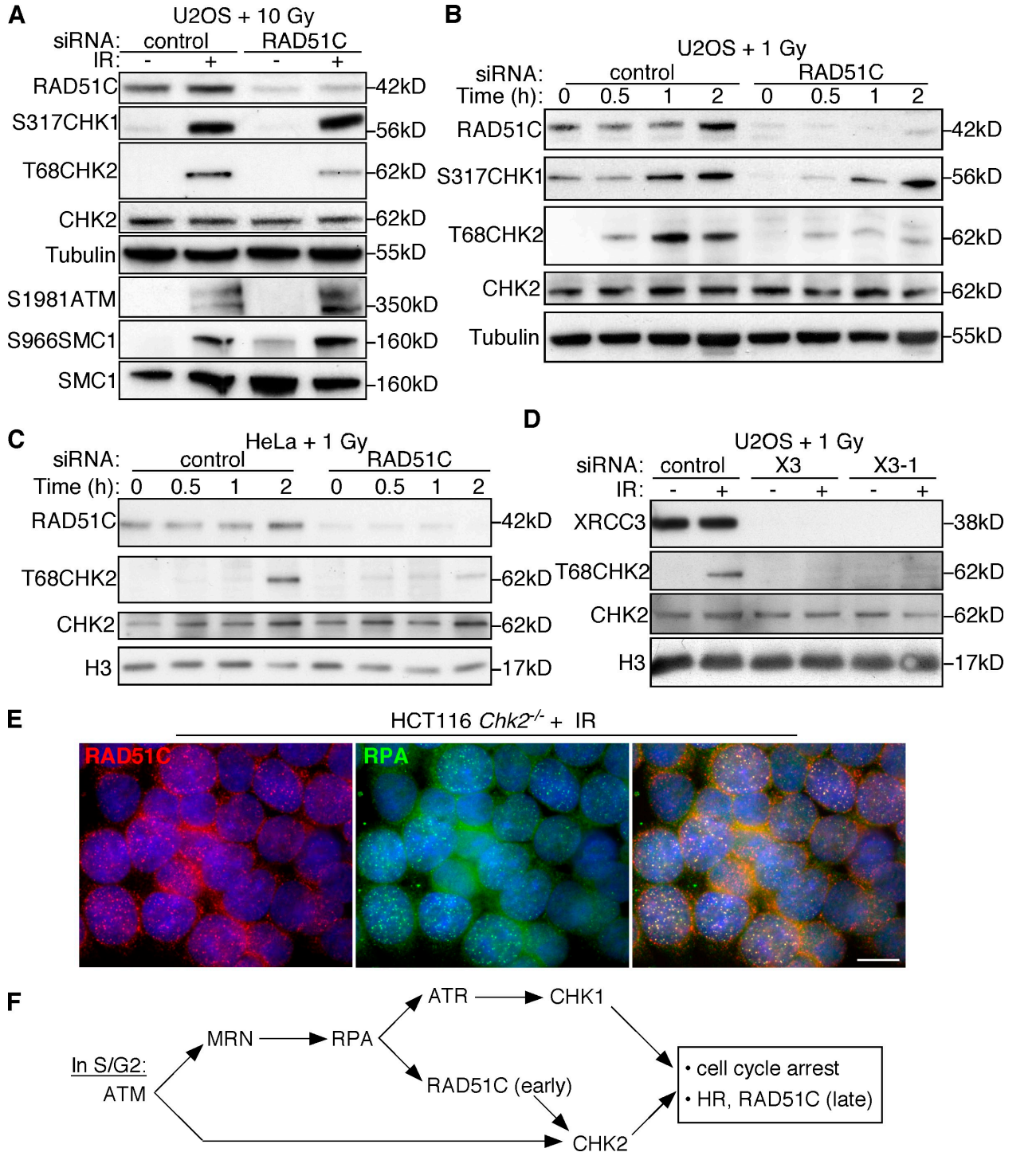

Figure 7. **RAD51C is required for IR-induced CHK2 phosphorylation.** (A) U2OS cells were transfected with control or RAD51C siRNA and irradiated (10 Gy) 48 h after transfection. After 2 h, extracts were prepared and immunoblotted as indicated. (B) As in A, but cells were treated with 1 Gy of IR, and protein samples were analyzed after 0.5, 1, and 2 h. (C) As in B, but using HeLa cells. (D) U2OS cells were transfected with a control siRNA or two different siRNAs against XRCC3 and irradiated (1 Gy) 48 h after transfection. After 2 h, extracts were prepared and immunoblotted as indicated. (E) HCT116 *Chk2*$^{-/-}$ cells were treated with 10 Gy of irradiation and fixed 2 h after. Cells were stained with anti-RAD51C (red) and anti-RPA antibodies (green). (F) Model for RAD51C action in response to DSBs in S/G2. RAD51C is recruited by RPA to break sites, where it facilitates CHK2-mediated cell cycle arrest and assembly of the HR machinery. Bar, 10 µm.

mediator of RAD51 nucleoprotein complex assembly (Sigurdsson et al., 2001); (d) hXRCC3, an interacting partner of RAD51C, assembles at DSBs early during DNA repair (Forget et al., 2004). Consistent with this, it was reported recently that RAD51C interacts directly with RAD51 in human cells after etoposide treatment (Rodrigue et al., 2006). A substantial set of data also supports the idea that RAD51C acts at late HR stages, after the RAD51-mediated strand invasion reaction has been completed.

This includes (a) association of Holliday junction branch migration and resolution activity with RAD51C in human cell extracts (Liu et al., 2004), (b) reduced Holliday junction resolution activity in *Rad51c*-defective hamster cells and MEFs (Liu et al., 2004; Kuznetsov et al., 2007), (c) RAD51C–XRCC3 complex binding to Holliday junctions in vitro (Liu et al., 2007), (d) maintenance of RAD51C foci on mouse meiotic chromosomes at late prophase I stages, at the time of Holliday junction resolution (Liu et al., 2007), and (e) broken chromatids in mouse oocytes expressing a hypomorphic *Rad51c* allele in metaphase II, which is linked to a defect in meiotic Holliday junction resolution (Kuznetsov et al., 2007).

In this study, we have used a monoclonal antibody to characterize the behavior of hRAD51C at sites of radiation-induced DNA damage. RAD51C accumulates in nuclear foci, which identify sites of damage, as judged by the colocalization with other DNA repair proteins, RAD51 and RPA. Colocalization of RAD51C with RAD51 foci is only partial, which is consistent with overlapping but not coinciding functions for these proteins. The kinetics and dependencies of recruitment of the two proteins at break sites delineate an ordered assembly pathway (Fig. 7 F). RAD51C recruitment to break sites requires ATM and NBS1 activities involved in strand resection at DSBs as well as RPA, which decorates the ssDNA overhangs produced. In response to IR, RAD51C appears at break sites with roughly similar kinetics as RAD51 (Fig. 2 A). After release from HU-induced replication arrest, RAD51C foci appeared distinctly before RAD51, indicating that under these conditions RAD51C acts before recruitment of the recombinase. In *Brca2*-deficient cells, RAD51C foci form in response to radiation, whereas RAD51 fails to associate with damage sites. Therefore, we propose that, during the early stages of DNA break repair by HR, RAD51C, possibly alone or more likely in complex with other paralogues, acts as a platform for the assembly of RAD51 filaments from RAD51 monomers delivered to the DSB by BRCA2. Thereafter, although RAD51 dissociates again from the break sites as recombination reactions proceed, RAD51C persists for distinctly longer periods of time. Thus, RAD51C could act as a recruitment platform for postinvasion HR activities (i.e., Holliday junction branch migration and resolution) in the late stages of DSB repair. Of the five members of the RAD51 paralogue family, only RAD51C has been shown to be part of several subcomplexes: RAD51B–RAD51C–RAD51D–XRCC2, RAD51B–RAD51C, and RAD51C–XRCC3 (Masson et al., 2001; Sigurdsson et al., 2001; Wiese et al., 2002). It is not clear from our current experiments whether RAD51C associates with DSBs continuously throughout repair or whether there is an early and a late wave of distinct RAD51C-containing protein complex assembly at break sites. Answers to this question await the availability of higher sensitivity antibodies against other members of the RAD51 paralogue family.

A role for RAD51C in DNA damage signaling

Previous studies suggested the possibility that the early role of RAD51C in DNA repair is that of facilitating assembly of RAD51 filaments at sites of DNA damage (Takata et al., 2001; French et al., 2002; Rodrigue et al., 2006). In this study, we demonstrate that, in addition to promoting RAD51 assembly, RAD51C is required for efficient checkpoint signaling to delay cell cycle progression in response to DNA damage. This function is shared between RAD51C and RPA, and we find that both proteins assemble in coinciding foci at sites of damage, specifically during S/G2 phase of the cell cycle. RPA foci form in the absence of RAD51C, suggesting that strand resection activities and RPA association with ssDNA do not require RAD51C. Conversely, RAD51C relies on RPA for its assembly at the break. This indicates that RAD51C requires RPA to mediate its association with the break site.

RPA-coated ssDNA is generated in an ATM-dependent manner (Jazayeri et al., 2006) and facilitates recruitment of the ATR–ATR-interacting protein complex (Zou and Elledge, 2003), leading to phosphorylation of the CHK1 checkpoint effector kinase. In this study, we report that RAD51C plays a similar role in checkpoint signaling by promoting phosphorylation and thereby activation of the CHK2 kinase. This role is shared by XRCC3, which is also a member of the RAD51 paralogue family and interacting partner of RAD51C. Both ATM and NBS1 are required for CHK2 phosphorylation in vivo (Matsuoka et al., 1998; Buscemi et al., 2001; Falck et al., 2001), and ATM has the ability to directly phosphorylate CHK2 in vitro (Matsuoka et al., 2000). RAD51C is also regulated by both factors, and potential ATM phosphorylation sites have been identified (Matsuoka et al., 2007). Whether RAD51C is a target for ATM phosphorylation remains to be investigated.

It is interesting to note that RAD51C is recruited to DNA break sites only in the S/G2 phase of the cell cycle. This is consistent with CHK2 activation in response to DNA damage during G1 occurring independently of RAD51C. Indeed, in vitro reconstitution experiments suggest that the MRN complex is sufficient to promote ATM activation and CHK2 phosphorylation at paired duplex DNA ends. Such ends likely model DNA breaks in G1, which is consistent with the observation that CHK2 is phosphorylated in response to DNA damage in G1 (Matsuoka et al., 1998; Lee and Paull, 2005). In experiments using a cell-free extract system, Shiotani and Zou (2009) have demonstrated that 3′ ssDNA overhangs, as generated during DNA break processing in S/G2, are inhibitory to ATM activation and CHK2 phosphorylation when compared with unprocessed ends. Therefore, it is conceivable that, in vivo during the S/G2 phases of the cell cycle, additional factors act at DNA ends to promote the generation and/or propagation of the checkpoint signal. Our results identify RAD51C as one such factor with a role in transduction of the checkpoint signal to CHK2. How RAD51C acts at DNA break sites to achieve this is an interesting question for future studies. It is possible that such a role could be direct, with RAD51C acting to recruit or mediate recruitment of canonical checkpoint proteins. Alternatively, it is possible that RAD51C plays an indirect role, being required for structural chromatin changes at the break site that allow efficient generation or propagation of the checkpoint signal. Both could be consistent with a more pronounced requirement for RAD51C at low IR doses.

An important implication of our results is that RAD51C controls RAD51 filament and HR activation at multiple levels,

the earliest of which is by modulating the DNA damage signal emanating from DSBs, which halts cell cycle progression and reduces Cdk activity. In turn, this allows BRCA2 to interact with RAD51 and engage the RPA-coated ssDNA in HR reactions leading to repair (Jazayeri et al., 2006). In support of this model, we observed similar cell cycle regulation of IR-induced RAD51C, RPA, and RAD51 focus formation, all being restricted to S and G2 (Yuan et al., 2003; unpublished data).

The cell cycle arrest defect observed in RAD51C-depleted cells in response to IR could be explained by reduced CHK2 phosphorylation. CHK2 is phosphorylated in both S and G2 cells exposed to IR and controls the intra-S checkpoint (Falck et al., 2001) as well as Cdk activity required for the G2/M transition (Matsuoka et al., 1998). Consistent with RAD51C-dependent regulation of CHK2 activation, we observe both a less robust S-phase delay and an increase in the fraction of cells entering mitosis 2 h after DNA damage. RAD51C-defective cells accumulate endogenous DNA damage and enter mitosis with unrepaired DSBs, most likely as the result of defective CHK2-dependent checkpoint control at the G2/M transition. Conversely, RAD51C accumulation at sites of damage seems unaffected by the absence of CHK2. Furthermore, RAD51C function in checkpoint mediation appears independent of RAD51 filament assembly, as lack of RAD51 does not affect integrity of the CHK2 checkpoint. Together, our data support a role for RAD51C as a mediator in the early steps of DNA damage signaling (Fig. 7 F) in addition to its role in promoting HR reactions at the break sites.

Materials and methods

Cell culture and treatments

HeLa 1.2.11 (Tarsounas et al., 2004b), U2OS, HCT116 wild-type, and *Chk2*$^{-/-}$ cells (a gift from F. Bunz, John Hopkins University, Baltimore, MD; Jallepalli et al., 2003), and NBS1 LB1 cells infected with pLPC-NBS1 or pLPC (a gift from M. Zdziencka, University of Leiden, Leiden, Netherlands; Kraakman-van der Zwet et al., 1999) were cultivated in monolayers in Dulbecco's minimum essential medium (Invitrogen) supplemented with antibiotics (penicillin and streptomycin; Sigma-Aldrich) and 10% FBS (Invitrogen). Ataxia telangiectasia fibroblasts transduced with empty vector or ATM (GM16666 and GM16667, respectively; Coriell Institute Repository) were grown under similar conditions except that medium was supplemented with 15% FBS. Human CAPAN-1 cells were cultivated in 2% RPMI medium supplemented with 15% FBS.

Single-cell clones were established as previously described (Bekker-Jensen et al., 2006). In brief, U2OS cell lines stably expressing GFP-RAD51C (a gift from J.-Y. Masson, Laval University Cancer Research Center, Quebec City, Quebec, Canada) or RAD51C* were generated by transfecting the expression construct alone (RAD51C*) or together with the pBabe–puro construct. After selection with 3 µg/ml puromycin for 14 d, single-cell clones were derived by serial dilutions in 96-well plates and tested for expression of the target protein.

γ irradiation was performed using a ^{137}Cs source at the dose indicated. The ATM inhibitor Ku55933 (a gift from G. Smith, AstraZeneca, Manchester, England, UK; Hickson et al., 2004) was added at 10-µM final concentration for 30 min before irradiation. Caffeine (Sigma-Aldrich) was added at 5-mM final concentration 2 h before irradiation. For HU treatment, cells were incubated 8–12 h after seeding with 2 mM HU for 17 h. Then, cells were incubated with fresh medium for the indicated period of time. For the 1.5 keV ultrasoft x-ray irradiation, cells were plated on the 0.9-µm thick Mylar base of an irradiation dish. The dish was placed in contact with an irradiation mask patterned with a 1-µm thick gold grid, through which the cells were irradiated. The grid consists of a series of 9-µm wide stripes separated by 1-µm gaps, resulting in cells being irradiated with a series of 1-µm stripes at 10-µm intervals.

Immunofluorescence

For indirect immunofluorescence staining, cells were seeded onto coverslips 24 h before irradiation. When CAPAN-1 cells were used, coverslips were coated with a solution of 0.1 mg/ml fibronectin before plating the cells. After irradiation, cells were allowed to recover for the indicated times, washed in PBS, and swollen in hypotonic solution (85.5 mM NaCl and 5 mM $MgCl_2$, adjusted to pH 7.0) for 5 min. For ultrasoft x ray–treated cells, 0.1% Triton X-100 was added to the hypotonic solution. Cells were fixed with 4% paraformaldehyde for 10 min at room temperature, permeabilized by adding 0.03% SDS to the fixative, and immunostained as described previously (Tarsounas et al., 2003). For time point collection, cells were kept in PBS on ice for up to 2 h before processing. Dried coverslips were mounted on microscope slides using the ProLong Antifade kit (Invitrogen) supplemented with 1 µg/ml DAPI. Specimens were viewed with an inverted microscope (DMI6000B; Leica) and fluorescence imaging workstation equipped with an HCX Plan-Apochromat 100× NA 1.4-0.7 oil objective, and images were acquired at room temperature using a digital camera (DFC350 FX R2; Leica) using LAS-AF software (Leica). Brightness and contrast adjustments were applied to the whole image using Photoshop CS3 (Adobe).

Immunoblotting

Cells were harvested by trypsinization, washed once with cold HBSS, and resuspended in cold buffer A (10 mM Hepes, pH 7.9, 10 mM KCl, 1.5 mM $MgCl_2$, 0.3 M sucrose, 10% glycerol, 1 mM DTT, and 0.05% Triton X-100) supplemented with protease and phosphatase inhibitor cocktail tablets (Roche) at a concentration of 2×10^7 cells/ml. After extraction on ice for 5 min, the cell suspension was cleared by centrifugation at maximum speed in a bench-top centrifuge (model 5424; Eppendorf). The nuclear pellet was resuspended in SDS-PAGE loading buffer and sonicated. Equal amounts of protein (50–100 µg) were analyzed by gel electrophoresis followed by Western blotting. NuPAGE-Novex 10% Bis-Tris and 10% Tris-Gly gels (Invitrogen) were run according to the manufacturer's instructions. Antitubulin, anti–histone H3, or anti–histone H2AX antibody was used for a loading control.

Antibodies

Mouse monoclonal antibodies 2H11 raised against hRAD51C, 10F1 raised against human XRCC3, 3E1 raised against GFP, and TAT-1 raised against α-tubulin (Masson et al., 2001; Tarsounas et al., 2004b) were obtained from the Cancer Research UK monoclonal antibody service. Mouse IgGs were purified from hybridoma supernatants using Gentle Ag/Ab Elution Buffer (Thermo Fisher Scientific). Rabbit polyclonal antibodies were raised against full-length RAD51 (FBE2; Barlow et al., 1997) and the 70-kD subunit of RPA (SWE34; a gift from S. West, Cancer Research UK, Hertfordshire, England, UK). Additional antibodies used were anti-H2AX (EMD); anti–histone H3 (a gift from A. Verreault, University of Montréal, Montréal, Quebec, Canada); anti–CENP-F (Abcam); anti–phospho histone H3–Ser 10 (6G3), anti–phospho CHK1–Ser 317, anti–phospho CHK2–Thr 68, and anti-CHK2 (all from Cell Signaling Technology); anti–phospho CHK2 (R&D Systems); anti-CHK2/Cds1 (Millipore); and anti-SMC1 and anti–phospho SMC1–Ser 966 (Bethyl Laboratories, Inc.). The anti–mouse RAD51C rabbit serum MTA37 was generated against the N-terminal peptide RELVGYPLSPAVRGKGKLVAAGFQTAED. The serum was affinity purified using the peptide cross-linked to Sulfo Link gel (Thermo Fisher Scientific).

RNAi

HeLa and U2OS cells were transfected using Oligofectamine (Invitrogen). In brief, $0.2–0.5 \times 10^6$ cells/well of a 6-well plate were plated 24 h before transfection. Cells were transfected with 2 µg siRNA/well twice at 7-h time intervals and processed 48 h later. siRNA duplexes were 21 base pairs with a 2-base deoxynucleotide overhang (Thermo Fisher Scientific). The sequences of RAD51C siRNAs were 5′-CACCTTCTGTTCAGCACTAGA-3′ (51C siRNA; Rodrigue et al., 2006) and 5′-GAGAATGTCTCACAAATAA-3′ (51C-1 siRNA); the sequences of XRCC3 siRNAs were 5′-GAATTATTGCTGCAATTAA-3′ (X3 siRNA) and 5′-GCCAGATCTTCATCGAGCA-3′ (X3-1 siRNA; Rodrigue et al., 2006); the sequence of RPA siRNA was 5′-AACACTCTATCCTCTTTCATGTT-3′ (Zou and Elledge, 2003; McCabe et al., 2006); and the sequence of RAD51 siRNA was 5′-CTTTGGCCCACAACCCAT-3′. A GFP siRNA with the sequence 5′-GCTGACCCTGAAGTTCATCTT-3′ (Tarsounas et al., 2004b) was used as a control. For expression of siRNA-resistant RAD51C (RAD51C*), the plasmid pcDNA3-RAD51C was modified by site-directed mutagenesis as previously described (Rodrigue et al., 2006).

Computational RAD51 and RAD51C foci analysis

Image analysis was performed after acquisition using the TRI2 software package, based on the Compact Hough and Radial Map algorithms

(Barber et al., 2001, 2007). The algorithm was used to detect nuclei and then to count foci within the nuclei from images acquired using DAPI and Cy3 fluorescent channels.

G2/M checkpoint assay

The G2/M checkpoint assay was performed as previously described (Kolas et al., 2007). In brief, U2OS cells were transfected with control or RAD51C siRNA twice at 18-h time intervals, as described in RNAi, and, 48 h later, were exposed to 1 Gy of IR. After 2 h, cells were harvested, washed twice in PBS, and fixed in 1% paraformaldehyde at 37°C for 10 min. After permeabilization in ice-cold 90% methanol, cells were washed in PBS and stained with anti–phospho histone H3–Ser 10 antibody followed by Alexa Fluor 488–conjugated goat anti–mouse IgG secondary antibody (Invitrogen). Cells were incubated with 5 µg/ml propidium iodide and 0.25 mg/ml RNase I in PBS. At least 10,000 cells were analyzed by flow cytometry (BD Biosciences). Data were processed using CellQuest (BD Biosciences).

MEF retroviral transduction and metaphase preparation

Primary MEFs were isolated from day 13.5 embryos as previously described (Blasco et al., 1997) and cultivated in Dulbecco's minimum essential medium supplemented with antibiotics (penicillin and streptomycin) and 10% FBS. Retroviral transduction of primary MEFs was performed as previously described (Palmero and Serrano, 2001). In brief, HEK293T packaging cells were grown to 70% confluency and transfected with pRetroSuper-shRNA and pCL-Eco helper vector using a standard calcium phosphate protocol. The media was replaced 24 h after transfection. Recipient MEFs were plated and infected 24 h later with the retroviral supernatants produced by the HEK293T cells. Additional infections were performed after 24 and 36 h. 24 h after the last infection, cells were washed and incubated with fresh media containing 2 µg/ml puromycin for 48 h. Exponentially growing MEFs (obtained from A. Zelensky, Medical Research Council, Harwell, England, UK) were either collected and processed for Western blot analysis, as described in Immunoblotting, or incubated with 0.1 µg/ml colcemid (Invitrogen) for 4 h at 37°C and then fixed in methanol/acetic acid (3:1). FISH was performed as previously described (Tarsounas et al., 2004b) using 15 µg/ml Cy3-conjugated PNA[CCCTAA]$_3$ telomeric probe (Applied Biosystems), and chromosomes were visualized with DAPI.

Online supplemental material

Fig. S1 illustrates formation of RAD51C foci in response to increasing doses of irradiation. Fig. S2 demonstrates the specificity of the RAD51C monoclonal antibody and accumulation of GFP-RAD51C foci in nuclear stripes induced by partial irradiation of cells with ultrasoft x rays. Fig. S3 shows inhibition of IR-induced RAD51C foci by caffeine. Fig. S4 examines a possible physical interaction between RAD51C and RPA. Fig. S5 shows lack of CHK2 activation in irradiated U2OS cells depleted of RAD51C using a second siRNA (RAD51C-1) as well as in RAD51C-depleted MEFs and normal CHK2 activation in irradiated U2OS cells depleted of RAD51. Online supplemental material is available at http://www.jcb.org/cgi/content/full/jcb.200811079/DC1.

We are grateful for DNA constructs, antibodies, and cell lines provided by F. Bunz, J.-Y. Masson, A. Verreault, A. Windle, M. Zdziencka, S. West, and the Cancer Research UK cell services. We thank S. Townsend and M. Woodcock for assistance with FACS analysis, A. Zelensky for retrovirally infected MEFs, A. Carr and S. Jackson for discussions and advice, and F. Uhlmann for critical reading and comments on the manuscript.

This work was supported by Cancer Research UK.

Submitted: 14 November 2008
Accepted: 21 April 2009

References

Adams, K.E., A.L. Medhurst, D.A. Dart, and N.D. Lakin. 2006. Recruitment of ATR to sites of ionising radiation-induced DNA damage requires ATM and components of the MRN protein complex. *Oncogene*. 25:3894–3904.

Barber, P.R., B. Vojnovic, J. Kelly, C.R. Mayes, P. Boulton, M. Woodcock, and M.C. Joiner. 2001. Automated counting of mammalian cell colonies. *Phys. Med. Biol.* 46:63–76.

Barber, P.R., R.J. Locke, G.P. Pierce, K. Rothkamm, and B. Vojnovic. 2007. Gamma-H2AX foci counting: image processing and control software for high-content screening. *Proceedings of SPIE*. 6441:64411M.

Barlow, A.L., F.E. Benson, S.C. West, and M.A. Hultén. 1997. Distribution of Rad51 recombinase in human and mouse spermatocytes. *EMBO J.* 16:5207–5215.

Bartek, J., and J. Lukas. 2007. DNA damage checkpoints: from initiation to recovery or adaptation. *Curr. Opin. Cell Biol.* 19:238–245.

Bekker-Jensen, S., C. Lukas, R. Kitagawa, F. Melander, M.B. Kastan, J. Bartek, and J. Lukas. 2006. Spatial organization of the mammalian genome surveillance machinery in response to DNA strand breaks. *J. Cell Biol.* 173:195–206.

Bennett, B.T., and K.L. Knight. 2005. Cellular localization of human Rad51C and regulation of ubiquitin-mediated proteolysis of Rad51. *J. Cell. Biochem.* 96:1095–1109.

Blasco, M.A., H.W. Lee, P.M. Hande, E. Samper, P.M. Lansdorp, R.A. DePinho, and C.W. Greider. 1997. Telomere shortening and tumor formation by mouse cells lacking telomerase RNA. *Cell*. 91:25–34.

Buscemi, G., C. Savio, L. Zannini, F. Miccichè, D. Masnada, M. Nakanishi, H. Tauchi, K. Komatsu, S. Mizutani, K. Khanna, et al. 2001. Chk2 activation dependence on Nbs1 after DNA damage. *Mol. Cell. Biol.* 21:5214–5222.

Chen, J., D.P. Silver, D. Walpita, S.B. Cantor, A.F. Gazdar, G. Tomlinson, F.J. Couch, B.L. Weber, T. Ashley, D.M. Livingston, and R. Scully. 1998a. Stable interaction between the products of the BRCA1 and BRCA2 tumor suppressor genes in mitotic and meiotic cells. *Mol. Cell*. 2:317–328.

Chen, P.L., C.F. Chen, Y.M. Chen, J. Xiao, Z.D. Sharp, and W.H. Lee. 1998b. The BRC repeats in BRCA2 are critical for Rad51 binding and resistance to methyl methanesulfonate treatment. *Proc. Natl. Acad. Sci. USA*. 95:5287–5292.

Cuadrado, M., B. Martinez-Pastor, M. Murga, L.I. Toledo, P. Gutierrez-Martinez, E. Lopez, and O. Fernandez-Capetillo. 2006. ATM regulates ATR chromatin loading in response to DNA double-strand breaks. *J. Exp. Med.* 203:297–303.

Davies, A.A., J.-Y. Masson, M.J. McIlwraith, A.Z. Stasiak, A. Stasiak, A.R. Venkitaraman, and S.C. West. 2001. Role of BRCA2 in control of the RAD51 recombination and DNA repair protein. *Mol. Cell*. 7:273–282.

Falck, J., N. Mailand, R.G. Syljuasen, J. Bartek, and J. Lukas. 2001. The ATM-Chk2-Cdc25A checkpoint pathway guards against radioresistant DNA synthesis. *Nature*. 410:842–847.

Fletcher, L., T.J. Yen, and R.J. Muschel. 2003. DNA damage in HeLa cells induced arrest at a discrete point in G2 phase as defined by CENP-F localization. *Radiat. Res.* 159:604–611.

Forget, A.L., B.T. Bennett, and K.L. Knight. 2004. Xrcc3 is recruited to DNA double strand breaks early and independent of Rad51. *J. Cell. Biochem.* 93:429–436.

French, C.A., J.-Y. Masson, C.S. Griffin, P. O'Regan, S.C. West, and J. Thacker. 2002. Role of mammalian RAD51L2 (RAD51C) in recombination and genome stability. *J. Biol. Chem.* 277:19322–19330.

Garcia-Muse, T., and S.J. Boulton. 2005. Distinct modes of ATR activation after replication stress and DNA double-strand breaks in *Caenorhabditis elegans*. *EMBO J.* 24:4345–4355.

Godthelp, B.C., F. Artwert, H. Joenje, and M.Z. Zdzienicka. 2002. Impaired DNA damage-induced nuclear RAD51 foci formation uniquely characterizes Fanconi anemia group D1. *Oncogene*. 21:5002–5005.

Goggins, M., M. Schutte, J. Lu, C.A. Moskaluk, C.L. Weinstein, G.M. Petersen, C.J. Yeo, C.E. Jackson, H.T. Lynch, R.H. Hruban, and S.E. Kern. 1996. Germline BRCA2 gene mutations in patients with apparently sporadic pancreatic carcinomas. *Cancer Res.* 56:5360–5364.

Griffin, C.S., P.J. Simpson, C.R. Wilson, and J. Thacker. 2000. Mammalian recombination-repair genes XRCC2 and XRCC3 promote correct chromosome segregation. *Nat. Cell Biol.* 2:757–761.

Haaf, T., E.I. Golub, G. Reddy, C.M. Radding, and D.C. Ward. 1995. Nuclear foci of mammalian Rad51 recombination protein in somatic cells after DNA damage and its localization in synaptonemal complexes. *Proc. Natl. Acad. Sci. USA*. 92:2298–2302.

Hickson, I., Y. Zhao, C.J. Richardson, S.J. Green, N.M.B. Martin, A.I. Orr, P.M. Reaper, S.P. Jackson, N.J. Curtin, and G.C.M. Smith. 2004. Identification and characterization of a novel and specific inhibitor of the ataxia-telangiectasia mutated kinase ATM. *Cancer Res.* 64:9152–9159.

Jallepalli, P.V., C. Lengauer, B. Volgestein, and F. Bunz. 2003. The Chk2 tumor suppressor is not required for p53 responses in human cancer cells. *J. Biol. Chem.* 278:20475–20479.

Jazayeri, A., J. Falck, C. Lukas, J. Bartek, G.C.M. Smith, J. Lukas, and S.P. Jackson. 2006. ATM- and cell cycle-dependent regulation of ATR in response to DNA double-strand breaks. *Nat. Cell Biol.* 8:37–45.

Kolas, N.K., J.R. Chapman, S. Nakada, J. Ylanko, R. Chahwan, F.D. Sweeney, S. Panier, M. Mendez, J. Wildenhain, T.M. Thomson, et al. 2007. Orchestration of the DNA-damage response by the RNF8 ubiquitin ligase. *Science*. 318:1637–1640.

Kraakman-van der Zwet, M., W.J. Overkamp, A.A. Friedl, B. Klein, G.W. Verhaegh, N.G. Jaspers, A.T. Midro, F. Eckardt-Schupp, P.H. Lohman, and M.Z. Zdzienicka. 1999. Immortalization and characterization of Nijmegen Breakage syndrome fibroblasts. *Mutat. Res.* 434:17–27.

Kuznetsov, S., M. Pellegrini, K. Shuda, O. Fernandez-Capetillo, Y. Liu, B.K. Martin, S. Burkett, E. Southon, D. Pati, L. Tessarollo, et al. 2007. RAD51C deficiency in mice results in early prophase I arrest in males and sister chromatid separation at metaphase II in females. *J. Cell Biol.* 176:581–592.

Lee, J.-H., and T. Paull. 2005. ATM activation by DNA double-strand breaks through the Mre11-Rad50-Nbs1 complex. *Science*. 308:551–554.

Liu, N., J.E. Lamerdin, R.S. Tebbs, D. Schild, J.D. Tucker, M.R. Shen, K.W. Brookman, M.J. Siciliano, C.A. Walter, W.F. Fan, et al. 1998. Xrcc2 and Xrcc3, new human Rad51-family members, promote chromosome stability and protect against DNA cross-links and other damages. *Mol. Cell*. 1:783–793.

Liu, Y., J.-Y. Masson, R. Shah, P. O'Regan, and S.C. West. 2004. RAD51C is required for Holliday junction processing in mammalian cells. *Science*. 303:243–246.

Liu, Y., M. Tarsounas, P. O'Regan, and S.C. West. 2007. Role of RAD51C and XRCC3 in genetic recombination and DNA repair. *J. Biol. Chem.* 282:1973–1979.

Masson, J.-Y., M.C. Tarsounas, A.Z. Stasiak, A. Stasiak, R. Shah, M.J. McIlwraith, F.E. Benson, and S.C. West. 2001. Identification and purification of two distinct complexes containing the five RAD51 paralogs. *Genes Dev.* 15:3296–3307.

Matsuoka, S., M.X. Huang, and S.J. Elledge. 1998. Linkage of ATM to cell cycle regulation by the Chk2 protein kinase. *Science*. 282:1893–1897.

Matsuoka, S., G. Rotman, A. Ogawa, Y. Shiloh, K. Tamai, and S.J. Elledge. 2000. Ataxia telangiectasia-mutated phosphorylates Chk2 in vivo and in vitro. *Proc. Natl. Acad. Sci. USA*. 97:10389–10394.

Matsuoka, S., B.A. Ballif, A. Smogorzewska, E.R. McDonald III, K.E. Hurov, J. Luo, C.E. Bakalarski, Z. Zhao, N. Solimini, Y. Lerenthal, Y. Shiloh, S.P. Gygi, and S.J. Elledge. 2007. ATM and ATR substrate analysis reveals extensive protein networks responsive to DNA damage. *Science*. 316:1160–1166.

McCabe, N., N.C. Turner, C.J. Lord, K. Kluzek, A. Bialkowska, S. Swift, S. Giavara, M.J. O'Connor, A.N. Tutt, M.Z. Zdzienicka, et al. 2006. Deficiency in the repair of DNA damage by homologous recombination and sensitivity to poly(ADP-ribose) polymerase inhibition. *Cancer Res.* 66:8109–8115.

Miller, K.A., D.M. Yoshikawa, I.R. McConnell, R. Clark, D. Schild, and J.S. Albala. 2002. RAD51C interacts with RAD51B and is central to a larger protein complex in vivo exclusive of RAD51. *J. Biol. Chem.* 277:8406–8411.

Myers, J.S., and D. Cortez. 2006. Rapid activation of ATR by ionizing radiation requires ATM and Mre11. *J. Biol. Chem.* 281:9346–9350.

Palmero, I., and M. Serrano. 2001. Induction of senescence by oncogenic Ras. *Methods Enzymol.* 333:247–256.

Petrini, J.H.J., and T.H. Stracker. 2003. The cellular response to DNA double-strand breaks: defining the sensors and mediators. *Trends Cell Biol.* 13:458–462.

Renglin Lindh, A., N. Schultz, N. Saleh-Gohari, and T. Helleday. 2007. RAD51C (RAD51L2) is involved in maintaining centrosome number in mitosis. *Cytogenet. Genome Res.* 116:38–45.

Rodrigue, A., M. Lafrance, M.-C. Gauthier, D. McDonald, M. Hendzel, S.C. West, M. Jasin, and J.-Y. Masson. 2006. Interplay between human DNA repair proteins at a unique double-strand break in vivo. *EMBO J.* 25:222–231.

Scully, R., J.J. Chen, R.L. Ochs, K. Keegan, M. Hoekstra, J. Feunteun, and D.M. Livingston. 1997. Dynamic changes of BRCA1 subnuclear location and phosphorylation state are initiated by DNA damage. *Cell*. 90:425–435.

Shiloh, Y. 2003. ATM and related protein kinases: safeguarding genome integrity. *Nat. Rev. Cancer*. 3:155–168.

Shiotani, B., and L. Zou. 2009. Single-stranded DNA orchestrates and ATM-to-ATR switch at DNA breaks. *Mol. Cell*. 33:547–558.

Sigurdsson, S., S. Van Komen, W. Bussen, D. Schild, J.S. Albala, and P. Sung. 2001. Mediator function of the human RAD51B-RAD51C complex in RAD51/RPA-catalyzed DNA strand exchange. *Genes Dev.* 15:3308–3318.

Takata, M., M.S. Sasaki, E. Sonoda, T. Fukushima, C. Morrison, J.S. Albala, S.M.A. Swagemakers, R. Kanaar, L.H. Thompson, and S. Takeda. 2000. The RAD51 paralog Rad51B promotes homologous recombinational repair. *Mol. Cell. Biol.* 20:6476–6482.

Takata, M., M.S. Sasaki, S. Tachiiri, T. Fukushima, E. Sonoda, D. Schild, L.H. Thompson, and S. Takeda. 2001. Chromosome instability and defective recombinational repair in knockout mutants of the five Rad51 paralogs. *Mol. Cell. Biol.* 21:2858–2866.

Tarsounas, M., D. Davies, and S.C. West. 2003. BRCA2-dependent and independent formation of RAD51 nuclear foci. *Oncogene*. 22:1115–1123.

Tarsounas, M., A.A. Davies, and S.C. West. 2004a. RAD51 localization and activation following DNA damage. *Philos. Trans. R. Soc. Lond. B Biol. Sci.* 359:87–93.

Tarsounas, M., P. Muñoz, A. Claas, P.G. Smiraldo, D.L. Pittman, M.A. Blasco, and S.C. West. 2004b. Telomere maintenance requires the RAD51D recombination/repair protein. *Cell*. 117:337–347.

West, S.C. 2003. Molecular views of recombination proteins and their control. *Nat. Rev. Mol. Cell Biol.* 4:435–445.

Wiese, C., D.W. Collins, J.S. Albala, L.H. Thompson, A. Kronenberg, and D. Schild. 2002. Interactions involving the Rad51 paralogs Rad51C and XRCC3 in human cells. *Nucleic Acids Res.* 30:1001–1008.

Wong, A.K.C., R. Pero, P.A. Ormonde, S.V. Tavtigian, and P.L. Bartel. 1997. Rad51 interacts with the evolutionarily conserved BRC motifs in the human breast cancer susceptibility gene BRCA2. *J. Biol. Chem.* 272:31941–31944.

Yuan, S.-S.F., S.-Y. Lee, G. Chen, M. Song, G.E. Tomlinson, and E.Y. Lee. 1999. BRCA2 is required for ionizing radiation-induced assembly of Rad51 complex in vivo. *Cancer Res.* 59:3547–3551.

Yuan, S.S., H.L. Chang, and E.Y. Lee. 2003. Ionizing radiation-induced Rad51 nuclear focus formation is cell cycle-regulated and defective in both ATM(−/−) and c-Abl(−/−) cells. *Mutat. Res.* 525:85–92.

Zou, L., and S.J. Elledge. 2003. Sensing DNA damage through ATRIP recognition of RPA-ssDNA complexes. *Science*. 300:1542–1548.